Original Article

Characterization of parallel-hole collimator using Monte Carlo Simulation

Anil Kumar Pandey, Sanjay Kumar Sharma, Sellam Karunanithi, Praveen Kumar, Chandrasekhar Bal, Rakesh Kumar

Department of Nuclear Medicine, All India Institute of Medical Sciences, New Delhi, India

ABSTRACT

Objective: Accuracy of *in vivo* activity quantification improves after the correction of penetrated and scattered photons. However, accurate assessment is not possible with physical experiment. We have used Monte Carlo Simulation to accurately assess the contribution of penetrated and scattered photons in the photopeak window. **Materials and Methods:** Simulations were performed with Simulation of Imaging Nuclear Detectors Monte Carlo Code. The simulations were set up in such a way that it provides geometric, penetration, and scatter components after each simulation and writes binary images to a data file. These components were analyzed graphically using Microsoft Excel (Microsoft Corporation, USA). Each binary image was imported in software (ImageJ) and logarithmic transformation was applied for visual assessment of image quality, plotting profile across the center of the images and calculating full width at half maximum (FWHM) in horizontal and vertical directions. **Results:** The geometric, penetration, and scatter at 140 keV for low-energy general-purpose were 93.20%, 4.13%, 2.67% respectively. Similarly, geometric, penetration, and scatter at 140 keV for low-energy high-resolution (LEHR), medium-energy general-purpose (MEGP), and high-energy general-purpose (HEGP) collimator were (94.06%, 3.39%, 2.55%), (96.42%, 1.52%, 2.06%), and (96.70%, 1.45%, 1.85%), respectively. For MEGP collimator at 245 keV photon and for HEGP collimator at 364 keV were 89.10%, 7.08%, 3.82% and 67.78%, 18.63%, 13.59%, respectively. **Conclusion:** Low-energy general-purpose and LEHR collimator is best to image 140 keV photon. HEGP can be used for 245 keV and 364 keV; however, correction for penetration and scatter must be applied if one is interested to quantify the *in vivo* activity of energy 364 keV. Due to heavy penetration and scattering, 511 keV photons should not be imaged with HEGP collimator.

Keywords: Collimator, Monte Carlo Simulation, parallel-hole

INTRODUCTION

In order to improve photon statistics in the image, photopeak window is widened, thus the contribution of penetrated and scattered photons are included in the image. The geometric components of the photons are the photons which were detected without interaction inside the collimator. Gamma camera cannot classify the image forming photons into geometric, penetrated, or scattered photons. Therefore, with measuring the radio-activity, we cannot accurately characterize the collimator which includes the accurate assessment of penetrated and scattered photons.

Access this article online

Quick Response Code:

Website: www.ijnm.in

DOI: 10.4103/0972-3919.152974

Single-photon emission computed tomography images are reconstructed on the assumption that detected photons are those photons which are emitted from a source located in a pixel area (rectangular area of constant width) and entered the collimator hole parallel to the hole axis. These criteria are only achieved if the collimator hole have infinite length and infinitely small hole size. Parallel-hole collimator has finite length and finite hole size and, therefore, the detected photons are from the area enclosed by a cone whose vertex is at the point of interaction site of the photon on the crystal. In this case, the number of detected photons increases with the distance of the source from the collimator encompassing more area and therefore spatial resolution decreases. Moreover, photons entering the collimator hole at small angle can be detected after penetrating the septa and/or scattering inside the collimator and introduces error in the quantification of *in vivo* activity and results in reduced image contrast.

It is possible to track and record the life history of the individual photon originating from the source that ultimately deposits its

Address for correspondence:
Dr. Rakesh Kumar, E-81, Ansari Nagar (East), AIIMS Campus, New Delhi - 110 029, India.
E-mail: rkphulia@yahoo.com

complete energy inside the crystal using Monte Carlo Simulation. Therefore, with the help of Monte Carlo Simulation technique, accurate assessment of the geometric, penetration and scatter contribution inside the photopeak window can be made. The aim of the study was to estimate the geometric, penetration, and scatter components for parallel-hole collimators using Simulation of Imaging Nuclear Detectors (SIMIND) Monte Carlo Simulation code.

MATERIALS AND METHODS

In order to characterize the parallel-hole collimators we simulated the Millennium VG high-performance dual head gamma camera equipped with advanced XP digital detector GE Medical Systems, Milwaukee, WI, USA. having 1 inch NaI (Tl) crystal thickness, intrinsic spatial resolution of 0.450 cm and energy resolution of 8.80% at 140 keV. The dimension of the crystal was 500 × 400 mm. The parallel-hole collimators used was VG low-energy general-purpose (LEGP), low-energy high-resolution (LEHR), medium-energy general-purpose (MEGP) and high-energy general-purpose (HEGP) collimators. The collimator data used during the simulation are given in Table 1.

We have used the SIMIND V4.9f Monte Carlo code developed by Professor Michael Ljungberg.[1,2] We installed it on a personal computer having Windows 7 Home Basic (copyright© 2009 Microsoft Corporation) 64-bit operating system, 2 GB RAM and Intel (R) core (TM) i3-2120 CPU @ 3.30 GHz processor.

A cylindrical horizontal source of dimension 0.002 × 0.002× 0.002 cm in a horizontal cylindrical phantom of size 22 × 30 × 22 cm was placed at the height of 12 cm from the detector. Acceptance angle of photons emitted towards the camera was set as 45°. A total of twenty simulations were made for four different collimators (LEGP, LEHR, MEGP, and HEGP) with five different energies (75, 140, 245, 364, and 511 keV) each. At each simulation, energy window settings were ± 20%. We have included the contribution of lead X-rays scatter photons inside the collimator. In each simulation, we collected 1000 million (1×10^9) photons. The pixel size in the simulated planar point source images was 0.340 cm, and they were stored in 128 × 128 matrix. The SIMIND code creates a binary matrix image having float values (real *4). The simulations were set up in such a way that during each simulation gamma photons must impinge on whole camera surface, and at the end of simulation SIMIND writes the value of each component (geometric, penetration, and scatter) and images in separate files.

We imported these images in ImageJ and applied logarithmic transformation before displaying for visual and/or quantitative analysis. A square ROI was placed as shown in Figure 1 so that it completely enclosed the point source then used a java plug-in FWHM[3] to calculated FWHM in both vertical and horizontal direction. The Java plug-in provided the value of FWHM in terms of number of pixels. The value of FWHM was converted into mm by multiplying the number of pixel by the pixel size.

Algorithm to assess geometric, penetrated and scattered photons

The authors of the SIMIND Monte Carlo code have used the delta scattering methods to sample the photons interaction through the collimators[4]. The path length of the photons has been sampled according to the equation 1.

$$P = -\ln(R)/\mu\max \quad (1)$$

Where ln is the natural logarithm, R is the sampled uniform random number, and μmax is the largest attenuation coefficient within the heterogeneous media.

The collimator can be considered as heterogeneous medium of air (0 g/cm^3) and lead. Therefore, the ratio of $\mu/\mu\max$ for the collimator will be either 0 or 1. In this case, it is only necessary to test whether the end point is within the collimator hole or not. It is not necessary to find the geometric coordinates of end point of the photon.

The algorithm they have used to assess geometric, penetrated and scattered photons is briefly summarized as follows:

- Step 1: Record the entrance point of the gamma photon on the collimator face.
- Step 2: Determine whether the entrance point is inside the collimator hole or in the lead septa based on a mathematical formula mentioned in the reference[4] and keep the record
- Step 3: Sample the path length of the photon using equation (1) and determine what will happen to the photon

Table 1: Collimator data used during the simulation study

Characteristics	LEGP	LEHR	MEGP	HEGP
Hole size X cm	0.190	0.150	0.300	0.400
Hole size Y cm	0.212	0.168	0.335	0.447
Distance between two holes: x-direction (cm)	0.020	0.020	0.105	0.180
Distance between two holes: y-direction (cm)	0.141	0.118	0.350	0.535
Displacement center hole: x-direction (cm)	0.105	0.085	0.203	0.290
Displacement center hole: y-direction (cm)	0.177	0.143	0.342	0.491
Collimator thickness (cm)	3.500	3.500	5.800	6.600
Hole shape	Hexagonal	Hexagonal	Hexagonal	Hexagonal
Type of collimation	PA	PA	PA	PA

LEGP: Low-energy general-purpose, LEHR: Low-energy high-resolution, MEGP: Medium-energy general-purpose, HEGP: High energy general-purpose, PA: Parallel-hole collimation

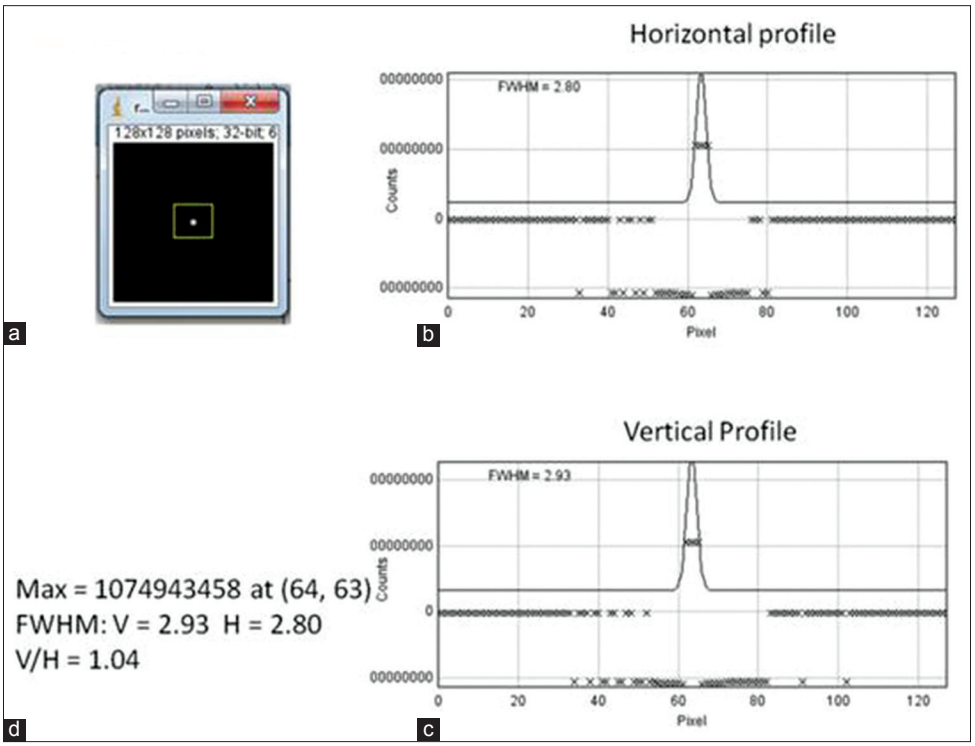

Figure 1: (a) Image of the point source with square ROI, (b) horizontal profile, (c) vertical profile and (d) result

at the end of the sampled path. If $R < \mu/\mu max$, then location is the final end point of the photon following the real interaction. Otherwise, continue tracking of photon by a new distance sampled according to equation (1). Record the number of interactions between the entrance point and final end point of the photon. The history of the gamma photon is terminated when all of their energy was absorbed within the collimator material or escaped from collimator.

- Step 4: Record the exit point on the collimator face towards NaI (Tl) crystal.
- Step 5: Compare the entrance and the exit points. If the entrance and exit point is inside the hole of the collimator, then flag the photon as the geometric photon. If some (one or more) interaction has occurred inside the lead material then flag the photon as scattered photons, otherwise flag the photon as the penetrated photon.
- Steps 6: Calculate the percentage of geometric, scattered and penetrated photons by dividing these numbers with the total number of photons that makes hits with the detector.
- Step 7: Geometric, scattered and penetrated photon when makes hit with detector, track them individually and sampled for their contribution in the photopeak window. Calculate the percentage of geometric, scattered, penetrated in the photopeak window by dividing with the total number of photopeak counts.

RESULTS

We evaluated the geometric, septal penetration, and scattering component in parallel-hole collimators (LEGP, LEHR, MEGP, and HEGP) using radio-active point source having energy ranging from 75 keV to 511 keV using Monte Carlo Simulation. The result of the simulation is given in Table 2. Figure 2 shows the variation of geometric, penetration, and scatter component with energy in LEGP, LEHR, MEGP, and HEGP collimators, respectively. Figure 3 shows images of point source obtained as a result of the simulation. It is clear that the geometric component has decreased with increase in energy, very sharp transition in case of LEGP and LEHR while comparatively smooth transition in MEGP and HEGP collimators [Figure 2]. Penetration and scatter component has increased with increase in energy showing sharp increase in case of LEGP and LEHR, with a smooth increase in MEGP and HEGP collimator.

Visual and quantitative assessment of the point source images

Image of the point source created at the end of each twenty simulation is shown in Figure 3. As shown in Figure 3, we have found the point source image superimposed on intense foggy background, and star artefacts (the camera-wide tails showing six-fold symmetry) resulting in the loss of image contrast. For a particular selection of collimator, the fogginess in the images has increased with increase in energy. This may be because of the selected higher energy photons to be imaged with respective collimators; at these energies respective collimators are becoming virtually transparent. This is evident from the calculated value of high septa penetration and scattering obtained as a result of the simulation in these selected combination of collimator and energy of the gamma photon shown in Table 2. It is important to note that Figure 3e, the foggiest image has the highest value of

Table 2: The result of the simulation

Collimator	Energy (keV)	Detector hits (absolute number of photons)	Geometric collimation (%)	Penetration (%)	Scatter in collimation (%)	Sum of penetration and scatter (%)
LEGP	75	25,176,678	90.78	2.81	6.42	9.23
LEGP	140	26,338,457	93.20	4.13	2.67	6.80
LEGP	245	55,636,957	5.75	68.52	25.73	94.25
LEGP	364	209,944,944	0.74	78.73	20.53	99.26
LEGP	511	415,029,460	0.34	84.96	14.70	99.66
LEHR	75	18,990,337	91.42	2.59	5.99	8.58
LEHR	140	19,794,520	94.06	3.39	2.55	5.94
LEHR	245	34,110,855	8.00	63.13	28.87	92.00
LEHR	364	146,624,963	0.68	74.99	24.32	99.31
LEHR	511	336,349,077	0.26	82.17	17.57	99.74
MEGP	75	17,879,513	93.26	1.21	5.53	6.74
MEGP	140	18,466,950	96.42	1.52	2.06	3.58
MEGP	245	19,396,882	89.10	7.08	3.82	10.90
MEGP	364	23,153,838	34.89	37.01	28.10	65.11
MEGP	511	32,644,005	4.55	57.95	37.51	95.46
HEGP	75	19,691,884	93.54	1.16	5.30	6.46
HEGP	140	20,358,953	96.70	1.45	1.85	3.30
HEGP	245	21,179,095	91.47	5.56	2.97	8.53
HEGP	364	23,074,365	67.78	18.63	13.59	32.22
HEGP	511	32,644,005	15.17	47.79	37.04	84.83

LEGP: Low-energy general-purpose, LEHR: Low-energy high-resolution, MEGP: Medium-energy general-purpose, HEGP: High energy general-purpose

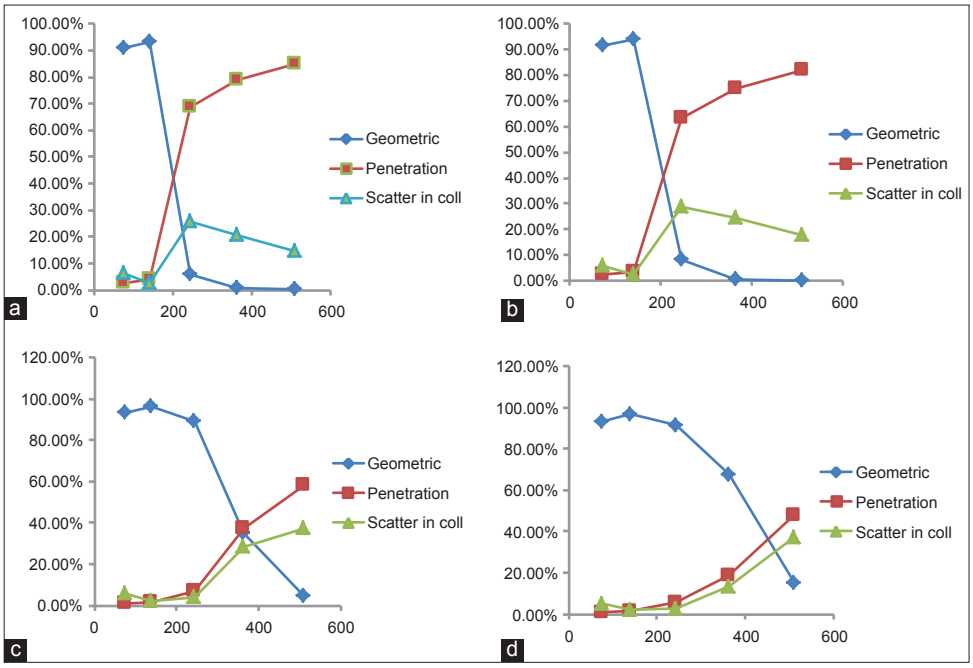

Figure 2: The variation of geometric, penetration, and scatter component with energy in low-energy general-purpose (a), low-energy high-resolution (b), medium-energy general-purpose (c) and high-energy general-purpose (d) collimators, respectively

penetration. The 6-fold symmetry of tails is associated with the hexagonal-hole shape of the collimator used in the simulation. The calculated vertical and horizontal FWHM on the images shown in Figure 3 is given in Table 3.

For a particular value of collimator, the FWHM of the point source (point spread function) have found to increase with increase in the energy, that is, with increase in energy, the system shows poorer spatial resolution. This may be due to increase in penetration and scatter inside the collimator with increase in photon energy. The spatial resolution (V = 9.962 mm and H = 9.52 mm at 140 keV) observed with LEHR collimator is best spatial resolution observed in this study. In this study we had selected two low-energy collimators (LEGP and LEHR), the better resolution of LEHR than that of LEGP may be due to smaller diameter of the holes (diameter = 0.150 cm, LEHR, and diameter = 0.190 cm, LEGP) [Table 2]. The spatial resolution observed at 140 keV for MEGP and HEGP in comparison to LEGP collimator may be due to combined effect of larger diameter of the holes (diameter = 0.300 cm

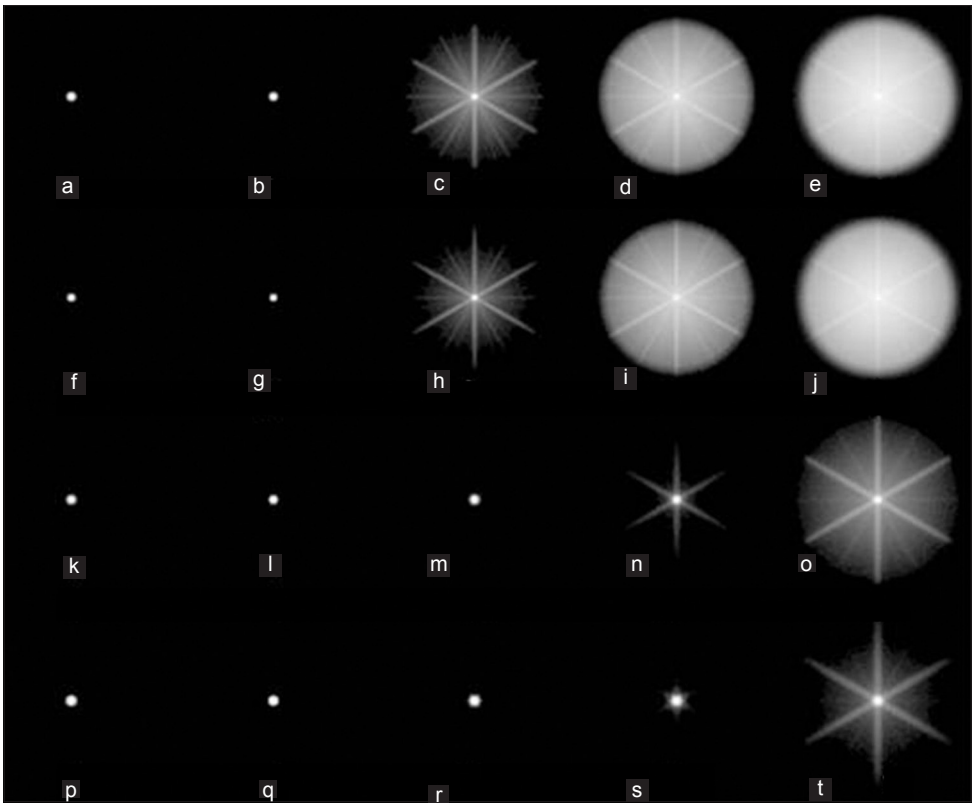

Figure 3: Image of the point source created at the end of each twenty simulation. Low-energy general-purpose (a-e), low-energy high-resolution (f-j), medium-energy general-purpose (k-o), high-energy general-purpose (p-t) images were simulated at 75 keV, 140 keV, 245 keV, 364 keV, and 511 keV, respectively

for MEGP and diameter = 0.400 cm for HEGP, increases sensitivity) and comparatively low percentage of scattered and penetrated components in case of MEGP and HEGP collimators (penetration and scatter = 6.80% for LEGP, 3.58% for MEGP, and 3.30% for HEGP) [Table 2].

DISCUSSION

The effect of penetration and scatter have been studied both qualitatively and quantitatively in clinical and phantom study and found that the accuracy of quantification improves by incorporating the compensation of collimator detecting response function.[5-15] The collimator detector response function has four component namely intrinsic response, geometric, penetration and scatter component of the collimator parameters. Accurate quantification of *in vivo* activity requires the assessment of the contribution of penetrated and scattered photons so that the correction can be made. We assessed these contributions using Monte Carlo Simulation.

Although the geometric component does not depend on the energy, for all the four investigated parallel-hole collimator we found the value of geometric component at 75 keV was less than that at 140 keV. This may be because the one inch crystal thickness (used in the simulation) is optimized for imaging radioisotope having energy more than 100–511 keV and gamma camera is optimized for 140 keV most widely used radioisotope in nuclear medicine. 75 keV photon will penetrate approximately half the distance than that of 140 keV and light will travel from that point to the end of the crystal to PMT. The amount of light reaching the PMT will be less due to absorption and scattering of light inside the NaI (Tl) crystal. Therefore, the photopeak efficiency will be less in case of 75 keV photons. This may be the reason for less geometric component for 75 keV in comparison to 140 keV. Low-energy photon (75 keV) can also undergo multiple Compton scattering and final photopeak absorption, and this will increase the photopeak counts. Both the phenomena, that is, multiple scattering leading to final photopeak absorption and diffusion of light over a longer path before reaching PMTs, also degrade the spatial resolution.[16] For all the four collimators, we have found more FWHM (less spatial resolution) in comparison to the 140 keV photon [Table 3].

The value of geometric component has decreased with increase in energy of the gamma photons with all the collimator. One inch crystal is sufficient to absorb all 140 keV gamma photon completely; however, it is not sufficient to stop all high energy photon above 245 keV. And, therefore, efficiency of one inch NaI (Tl) crystal is low. The low geometric component may be due to low efficiency of one inch crystal thickness used in the simulation. This result is in good agreement with the previous publications by Shafaei *et al.* they have estimated geometric, penetration, and scatter component for the energy range of 250–450 keV for DST-XLi dual-head gamma camera with HEGP collimator[17]. The poor spatial resolution was observed in the case of MEGP in comparison to LEHR and LEGP for

Table 3: FWHM of the point source images of Figure 3

Energy	FWHM (mm)	
	Vertical	Horizontal
LEGP		
75	12.206	13.226
140	17.476	15.266
245	30.294	42.67
364	−3,400,000,000	89.284
511	3,400,000,000	3,400,000,000
LEHR		
75	10.2	9.962
140	9.962	9.52
245	24.344	18.122
364	−3,400,000,000	−3,400,000,000
511	−3,400,000,000	137.224
MEGP		
75	14.212	14.382
140	13.566	13.634
245	11.05	14.994
364	11.798	11.764
511	11.764	11.288
HEGP		
75	14.62	14.484
140	13.6	13.838
245	15.13	15.028
364	18.156	17.544
511	17.85	17.238

FWHM: Full width at half maximum, LEGP: Low-energy general-purpose, LEHR: Low-energy high-resolution, MEGP: Medium-energy general-purpose, HEGP: High energy general-purpose

140 keV photon. It may be attributed to the larger hole diameter and increased septa thickness.

The septa thickness is designed to control the number of photons penetrating the septa and generally it is such that less than 5% penetrated photons are allowed. We have found less than 5% septa penetration in both LEHR and LEGP collimators which is in agreement with the general principle of designing collimators septa thickness for imaging low-energy isotope up to 140 keV energy. We have found very high value of septa penetration and scatter, at energy higher than 140 keV for LEGP and LEHR collimator so that it is advised not to use these collimators for imaging high energy radioisotopes. Septa penetration was found to be more than 5% for both the collimators designed to image medium-energy or high energy radioisotopes. For MEGP collimator designed to image 245 keV, the septa penetration was 5.43% and HEGP designed to image 364 keV photons, we have found the value of septa penetration as 18.63% which is quite high, the contribution due to penetration and scattering is equal to 32.22%. Therefore, correction for penetration and scattering becomes very important in case of I-131 imaging when we are interested in the quantification of *in vivo* I-131 activity.

The length of the collimator holes affects resolution and sensitivity. As holes are made longer, gamma rays that are not quite perpendicular to the collimator are more likely to be absorbed in the septa before they reach the scintillation crystal. For MEGP and HEGP collimator, the hole length is 5.800 cm and 6.000 cm respectively. Hole length are increasing to maintain the resolution and hole size is increasing to maintain the sensitivity. Hole size for MEGP and HEGP collimator are 0.300 cm and 0.400 cm, respectively. Septa thickness is also increased to reduce the septal penetration in these collimators at high energy.

The inaccuracy in the calculation of FWHM [S. No. 3, 4, 5, 8, 9, 10, 14, 15, 19, 20 in Table 3] was observed in case of all the combination of collimator and energy of photons listed in Table 3. The calculated FWHM is nearly same for MEGP collimator (approximately 11.55 mm, S. No. 13, 14, and 15). However, by looking at the Figure 2m-o, it is obvious that the calculated FWHM cannot be accepted. The second example is in case of HEGP collimator, the calculate FWHM value shows that HEGP collimator has better resolution for 511 keV in comparison to the 364 keV photons, that is not acceptable which is clear from the Figure 2s and t. This inaccuracy in calculation of FWHM may be attributed to heavy septa penetration and scattering inside the collimator that has introduced star artefacts. The plugin used to calculate FWHM fits a Gaussian function to a horizontal and vertical cut that is centered on the brightest point in the image and returns the FWHM of the function both in numerical and graphical formats.

There is an obvious star artefact in Figure 3n is due to septa penetration, it is clear from the figure that a bright line is passing vertically through the brightest point source, therefore, vertical profile have high value of FWHM, while no such line exists in the horizontal direction through the brightest points, therefore, horizontal FWHM will be much less in comparison to vertical FWHM.

When the contribution of penetration and scattering is very high, the image of a point source becomes very blurred and becomes very difficult to put ROI in order to quantify the activity. The gamma camera modeled in our study is not the same as other investigators; therefore, a quantitative comparison is not possible. However, there are few studies related with assessment of geometric, penetration, and scatter components. Dewaraja *et al.*[12] have also calculated geometric, penetration and scatter components of events within 20% window at 364 keV for point source in air and found 73% of the events in the photopeak window had either scattered or penetrated the collimator. They simulated for NaI (Tl) crystal of size 24 × 40 cm and 0.95 cm crystal thickness, HEGP collimator with square size hole = 3.54 mm, septa = 1 mm, thickness = 5.84 cm.

Shafaei *et al.*[17] simulated for 3/8 inch NaI (Tl) crystal thickness, energy resolution 9.8% at 140 keV, HEGP collimator hexagonal-hole, collimator thickness 5.4 cm, septa thickness 0.16 cm, and found 64% either penetration or scatter in the photopeak window.

We have found 32.22% of the event, the 20% photopeak window center at 364 keV either penetrated or scattered in the HEGP

collimator (hexagonal-hole, hole diameter = 0.447 cm, collimator thickness 6.60 cm, septa thickness 0.535 cm). And 65.11% of the event the 20% photopeak window center at 364 keV either penetrated or scattered in the MEGP collimator (hexagonal-hole, hole diameter = 0.335 cm, collimator thickness 5.80 cm, septa thickness 0.350 cm).

It is important to take into account the effect of backscatter from the PMTs and shielding material surrounding the crystal because these photons might re-enter into the crystal. De Vries *et al*.[18] have shown that a single slab of 66% Pyrex is sufficient to model backscatter. We have used a single slab of 5 cm thick Pyrex just below the crystal to include the effect of backscatter in the simulation.

CONCLUSION

Low-energy general-purpose and LEHR collimator is best to image 140 keV photon. HEGP can be used for 245 keV and 364 keV; however, correction for penetration and scatter must be applied if one is interested to quantify the *in vivo* activity of energy 364 keV. Due to heavy penetration and scattering, 511 keV photons should not be imaged with HEGP collimator. The result of this study can be used for optimal collimator design and development of new correction algorithm, because for evaluation and design of scatter correction algorithm, proper understanding of how the scattered photons are distributed and about its properties is required.

REFERENCES

1. Ljunberg M. The SIMIND Monte Carlo program. In: Ljungberg M, Strand SE, King MA, editors. Monte Carlo Calculation in Nuclear Medicine: Applications in Diagnostic Imaging. Bristol: IOP Publishing; 1998. p. 145-63.
2. Ljungberg M. The SIMIND Monte Carlo program Home Page. Available from: http://www2.msf.lu.se/simind/index.asp. [Last accessed on 2014 May 5].
3. Available from: http://www.umanitoba.ca/faculties/science/astronomy/jwest/plugins.html. [Last accessed on 2014 May 5].
4. Ljungberg M, Larsson A, Johansson L. A new collimator simulation in SIMIND based on the delta-scattering technique. IEEE Trans Nucl Sci 2005;52:1370-5.
5. Tsui BM, Zhao X, Frey EC, McCartney WH. Quantitative single-photon emission computed tomography: Basics and clinical considerations. Semin Nucl Med 1994;24:38-65.
6. Pretorius PH, King MA, Pan TS, de Vries DJ, Glick SJ, Byrne CL. Reducing the influence of the partial volume effect on SPECT activity quantitation with 3D modelling of spatial resolution in iterative reconstruction. Phys Med Biol 1998;43:407-20.
7. Kohli V, King MA, Tin-Su P, Glick SJ. Compensation for distance-dependent resolution in cardiac-perfusion SPECT: Impact on uniformity of wall counts and wall thickness. Nucl Sci IEEE Trans 1998;45:1104-10.
8. Pretorius PH, Gifford HC, Narayanan MV, Dahlberg ST, King MA. Comparison of detection accuracy of perfusion defects in SPECT for different reconstruction strategies using polar-map quantitation. Nucl Sci IEEE Trans 2003;50:1569-74.
9. Narayanan MV, King MA, Pretorius PH, Dahlberg ST, Spencer F, Simon E, *et al.* Human-observer receiver-operating-characteristic evaluation of attenuation, scatter, and resolution compensation strategies for Tc-99 m myocardial perfusion imaging. J Nucl Med 2003;44:1725-34.
10. Frey EC, Gilland KL, Tsui BM. Application of task-based measures of image quality to optimization and evaluation of three-dimensional reconstruction-based compensation methods in myocardial perfusion SPECT. IEEE Trans Med Imaging 2002;21:1040-50.
11. Xin He, Frey EC, Links JM, Gilland KL, Segars WP, Tsui BM. A mathematical observer study for the evaluation and optimization of compensation methods for Myocardial SPECT using a phantom population that realistically models patient variability. Nucl Sci IEEE Trans 2004;51:218-24.
12. Dewaraja YK, Ljungberg M, Koral KF. Characterization of scatter and penetration using Monte Carlo simulation in 131I imaging. J Nucl Med 2000;41:123-30.
13. Ljungberg M, Sjögreen K, Liu X, Frey E, Dewaraja Y, Strand SE. A 3-dimensional absorbed dose calculation method based on quantitative SPECT for radionuclide therapy: Evaluation for (131) I using Monte Carlo simulation. J Nucl Med 2002;43:1101-9.
14. Sankaran S, Frey EC, Gilland KL, Tsui BM. Optimum compensation method and filter cutoff frequency in myocardial SPECT: A human observer study. J Nucl Med 2002;43:432-8.
15. Gifford HC, King MA, Wells RG, Hawkins WG, Narayanan MV, Pretorius PH. LROC analysis of detector-response compensation in SPECT. IEEE Trans Med Imaging 2000;19:463-73.
16. Moore J, Zoursdakis G. Emission imaging: SPECT and PET. Biomedical Technology and Devices Handbook. Ch. 10. New York: CRC Press, LLC; 2004. p. 10-54.
17. Shafaei M, Ay MR, Sardari D, Dehestani, Zaidi H. Monte Carlo Assessment of Geometric, Scatter and Septal Penetration Components in DST-XLi HEGP Collimator, Sloten JV, Verdonck P, Nyssen M, Haueisen J, editors. ECIFMBE 2008, IFMBE Proceedings 22, 2008. p. 2479-89.
18. De Vries DJ, Moore SC, Zimmerman RE, Mueller SP, Friedland B, Lanza RC. Development and validation of a Monte Carlo simulation of photon transport in an Anger camera. IEEE Trans Med Imaging 1990;9:430-8.

How to cite this article: Pandey AK, Sharma SK, Karunanithi S, Kumar P, Bal C, Kumar R. Characterization of parallel-hole collimator using Monte Carlo Simulation. Indian J Nucl Med 2015;30:128-34.

Source of Support: Nil. **Conflict of Interest:** None declared.